Neutral Phosphine Complexes of Antimony(III) and Bismuth(III) Halides†

William Clegg,[a] Mark R. J. Elsegood,[a] Victoria Graham,[a] Nicholas C. Norman,*[,a] Nigel L. Pickett[a] and Kayumars Tavakkoli[b]

[a] *Department of Chemistry, The University of Newcastle upon Tyne, Newcastle upon Tyne NE1 7RU, UK*
[b] *Department of Chemistry, Science Laboratories, The University of Durham, South Road, Durham DH1 3LE, UK*

The reaction between $BiBr_3$ and PEt_3 has afforded crystals of the centrosymmetric, tetrameric complex $[Bi_4Br_{12}(PEt_3)_4]$ in which each bismuth centre is octahedrally co-ordinated and bonded to one phosphine ligand. An alternative structural arrangement for a monophosphine complex has been found in a PMe_3 complex of SbI_3, $[\{SbI_3(PMe_3)\}_x]$, which is polymeric although with μ-I bridges of two types between the antimony centres such that a description as a polymer of dimers is appropriate. In the bis(phosphine) complex of $BiBr_3$, $[Bi_2Br_6(PMe_3)_4]$, a centrosymmetric, edge-shared, bioctahedral structure is observed with *cis* phosphines occupying one axial and one equatorial site per bismuth centre. Similar structures have been observed for the dmpe complexes $[E_2Br_6(dmpe)_2]$ [E = Sb or Bi; dmpe = 1,2-bis(dimethylphosphino)ethane] and the factors affecting which structural isomer is adopted, in comparison with a range of transition metal complexes, have been discussed. An isomeric tetrameric form of $[SbBr_3(dmpe)]$ has also been isolated.

It would be difficult to overstate the importance of phosphine ligands in the chemistry of the transition metals, especially for low oxidation states and particularly for those elements on the right of the d block,[1] but phosphines as ligands feature much less prominently in the chemistry of the p-block elements and have only a very minor role as ligands towards s- and f-block elements. The situation with d-, s- and f-block elements is, perhaps, unsurprising since phosphines are generally thought of as soft bases and are therefore expected to be associated more commonly with soft acids (low oxidation state d block) than with hard acids (s- and f-block); for the p-block elements with soft or borderline acidity, however, a reasonable complex chemistry might be expected. Nevertheless, despite any such expectation, the chemistry of the p-block elements (particularly the heavier elements) in association with phosphine ligands remains largely undeveloped. Most of the known phosphine complexes are for the heavier Group 13 and 14 elements, particularly those of Ga^{III}, In^{III} and Sn^{IV} halides,[2] although relatively few have been structurally characterised. In the case of the heavier elements of Group 15, which is the focus of this paper, notable early work includes a report by Holmes and Bertaut[3] describing complexes of the type $[ECl_3(PMe_3)_n]$ (E = P, As or Sb; n = 1 or 2) and a later report by Summers and Sisler[4] which confirmed these formulations and reported additional ^1H NMR and conductivity data indicative of varying degrees of ionic behaviour. Only recently have any such compounds been structurally characterised, however, these being $[PMe_3H]^+{}_n[\{Bi_2Br_7(PMe_3)_2\}_n]^{n-}$ **1**,[5] $[Bi_2Br_6(PMe_3)_4]$ **2**[6] and $[Bi_2Br_6(PMe_2Ph)_2(OPMe_2Ph)_2]$ **3**[6] for bismuth, and $[(py)_2H][SbI_4(dmpe)]$ **4**[7] [py = pyridine, dmpe = 1,2-bis(dimethylphosphino)ethane], $[SbBr_2(PMe_3)\{Fe(CO)(PMe_3)(\eta\text{-}C_5H_5)\}]$ **5**[8] and $[Sb(PPh_3)Me\{W(CO)_5\}_2]$ **6**[9] for antimony.

Herein we describe the structures of six phosphine complexes of antimony(III) and bismuth(III) halides, one of which, **2**, was the subject of a preliminary communication,[6] and discuss some of these structures in relation to analogous transition metal complexes.

† *Supplementary data available:* see Instructions for Authors, *J. Chem. Soc., Dalton Trans.*, 1994, Issue 1, pp. xxiii–xxviii.

Results and Discussion

The reaction between $BiBr_3$ and two equivalents of PEt_3 in thf (tetrahydrofuran) afforded, after work-up, moderate yields of a yellowish green crystalline compound, analytical data for which were indicative of a likely 1:1 adduct with stoichiometry $BiBr_3(PEt_3)$. This formulation was confirmed by X-ray crystallography the results of which are shown in Fig. 1; selected bond lengths and angles are listed in Table 1 and atomic positional parameters are presented in Table 2. The molecular structure comprises a tetrameric association of $BiBr_3(PEt_3)$ units, *i.e.* $[Bi_4Br_{12}(PEt_3)_4]$ **7**, with crystallographic C_i symmetry in which there are two unique bismuth atoms each bonded to one phosphine and five bromines. One way in which we may view this structure is as two linked, edge-shared bioctahedral units, the overall structure being closely related to a common tetrameric form of antimony and bismuth halogeno-anion, *viz.* $[E_4X_{16}]^{4-}$ (E = Sb or Bi; X = Cl, Br or I), in which the phosphine ligand sites in **7** are occupied by halide (X).[10] If

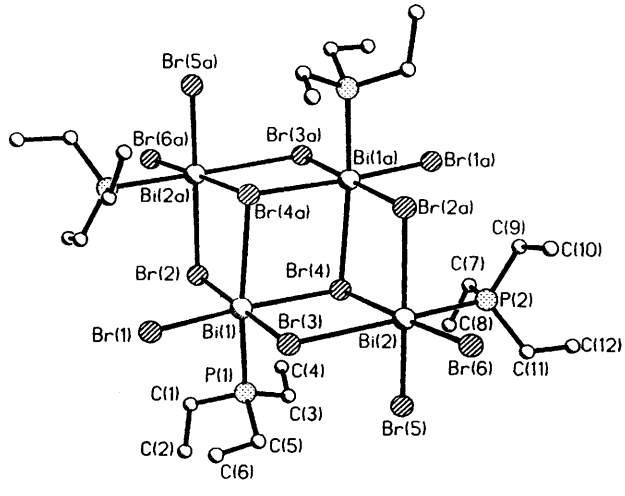

Fig. 1 A view of the molecular structure of **7**

we consider the crystallographically independent edge-shared bioctahedral fragment, Bi(1) is bonded to a phosphine [P(1)], one terminal bromine [Br(1)], two μ bromines [Br(3) and Br(2)] and two μ_3 bromines [Br(4) and Br(4a)]; the μ-Br(3) and μ_3-Br(4) act as bridges to Bi(2) within the same bioctahedral fragment, while μ-Br(2), μ_3-Br(4) and μ_3-Br(4a) serve as bridges to the centrosymmetrically related edge-shared bioctahedral fragment in the adjacent asymmetric unit. The Bi(2) atom is bonded to a phosphine [P(2)], two terminal bromines [Br(5) and Br(6)], two μ bromines [Br(3) and Br(2a)] and one μ_3 bromine [Br(4)].

The two Bi–P bond lengths [Bi(1)–P(1) 2.733(6) and Bi(2)–P(2) 2.747(7) Å] are similar to those found in **1**–**3** [**1**, 2.762(3); **2**, 2.865(3) and 2.716(3) (see later); **3**, 2.725(2) Å], lengths of this magnitude apparently being typical for a Bi–P co-ordinate bond for six-co-ordinate bismuth. With respect to the Bi–Br bond lengths, the terminal Bi–Br distances [2.691(3)–2.701(3) Å] are the shortest and within usual ranges. The Br(4) atom bridges Bi(1) and Bi(2) fairly symmetrically with somewhat longer Bi–Br distances [3.076(3) and 3.058(3) Å], but Br(3) is much more asymmetrically bound [2.776(3) and 3.313(4) Å] as a result of the lengthening of the Bi(2)–Br(3) bond which lies *trans* to P(2). This appreciable *trans* influence is probably the result of a strong interaction of the phosphorus lone pair with the *trans* Bi–Br σ* orbital, a bonding model we have commented upon in detail before.[11,12] The edge-shared bioctahedral units are linked by much longer bonds [Bi(1)–Br(4a) 3.302(3) and Bi(2)–Br(2a) 3.112(3) Å] than are present within the unit [with the exception of Bi(2)–Br(3) 3.313(4) Å], the longer of these being *trans* to the phosphine, P(2), as expected (see above). In terms of the co-ordination geometries, both bismuth centres are close to regular octahedral with no angles deviating from idealised values by more than 10°, and generally much less, which is indicative of Bi^{III} lone pairs with little stereochemical activity. This lack of stereochemical activity, at least as evidenced by marked deviations in bond angles from idealised values, is a usual feature of six-co-ordinate Bi^{III},[10] and a point to which we will return later.

An interesting structure for comparison with **7** is the phosphine sulfide complex $[Sb_4Br_{12}(SPMe_2Ph)_4]$[13] which has a very similar tetrameric structure but in which the phosphine sulfide ligands are in the bridging sites occupied, in **7**, by Br(2), Br(2a), Br(4) and Br(4a).

An alternative structural arrangement for a monophosphine adduct of the form $EX_3(PR_3)$ was encountered in a crystalline complex isolated from the reaction between SbI_3 and PMe_3 in thf. Yellow crystals obtained from this reaction were shown by X-ray crystallography to be a thf solvate with the empirical formula $[Sb_2I_6(PMe_3)_2]$·thf **8**; a view of part of the crystal structure is shown in Fig. 2, selected bond lengths and angles are given in Table 3 and atomic positional parameters are presented in Table 4. In contrast to the tetrameric nature of **7**, the structure of **8** is best described as a polymer of dimers, there being one unco-ordinated thf molecule of crystallisation per dimer unit (Fig. 2).

If we consider initially the dimeric unit $[Sb_2I_6(PMe_3)_2]$, each antimony has a square-based pyramidal co-ordination geometry with a PMe_3 ligand in the apical site and four iodines in the basal plane. The basal planes of the pyramids are then linked through an edge, defined by the vector between the bridging iodines I(1) and I(2), and with the apices having an *anti* configuration giving a dimeric structure with (non-crystallographic) C_{2h} symmetry. The integrity of this dimer as a crystallographically distinct unit can be gauged from the reasonably symmetric bridging nature of the iodines I(1) and I(2) evident from a consideration of the appropriate bond

Table 1 Selected bond lengths (Å) and angles (°) for **7***

Bi(1)–Br(1)	2.694(3)	Bi(1)–P(1)	2.733(6)
Bi(1)–Br(3)	2.776(3)	Bi(1)–Br(2)	2.928(3)
Bi(1)–Br(4)	3.076(3)	Bi(1)–Br(4a)	3.302(3)
Bi(2)–Br(5)	2.691(3)	Bi(2)–Br(6)	2.701(3)
Bi(2)–P(2)	2.747(7)	Bi(2)–Br(4)	3.058(3)
Bi(2)–Br(2a)	3.112(3)	Bi(2)–Br(3)	3.313(4)
Br(2)–Bi(2a)	3.112(3)		
Br(1)–Bi(1)–P(1)	88.72(13)	Br(1)–Bi(1)–Br(3)	90.61(9)
P(1)–Bi(1)–Br(3)	90.72(13)	Br(1)–Bi(1)–Br(2)	89.69(9)
P(1)–Bi(1)–Br(2)	88.77(13)	Br(3)–Bi(1)–Br(2)	179.40(7)
Br(1)–Bi(1)–Br(4)	176.35(7)	P(1)–Bi(1)–Br(4)	87.87(13)
Br(3)–Bi(1)–Br(4)	88.11(9)	Br(2)–Bi(1)–Br(4)	91.56(9)
Br(1)–Bi(1)–Br(4a)	101.00(7)	P(1)–Bi(1)–Br(4a)	167.89(13)
Br(3)–Bi(1)–Br(4a)	96.34(7)	Br(2)–Bi(1)–Br(4a)	84.12(6)
Br(4)–Bi(1)–Br(4a)	82.55(7)	Br(5)–Bi(2)–Br(6)	93.68(10)
Br(5)–Bi(2)–P(2)	89.2(2)	Br(6)–Bi(2)–P(2)	87.8(2)
Br(5)–Bi(2)–Br(4)	86.86(8)	Br(6)–Bi(2)–Br(4)	178.28(8)
P(2)–Bi(2)–Br(4)	90.6(2)	Br(5)–Bi(2)–Br(2a)	171.10(8)
Br(6)–Bi(2)–Br(2a)	93.99(9)	P(2)–Bi(2)–Br(2a)	86.6(2)
Br(4)–Bi(2)–Br(2a)	85.35(6)	Br(5)–Bi(2)–Br(3)	86.29(8)
Br(6)–Bi(2)–Br(3)	102.25(9)	P(2)–Bi(2)–Br(3)	169.28(14)
Br(4)–Bi(2)–Br(3)	79.41(8)	Br(2a)–Bi(2)–Br(3)	96.48(7)
Bi(1)–Br(2)–Bi(2a)	98.39(7)	Bi(1)–Br(3)–Bi(2)	96.39(9)
Bi(2)–Br(4)–Bi(1)	95.85(8)		

* Symmetry transformations used to generate equivalent atoms: a, $-x + 1, -y, -z + 1$.

Table 2 Atomic coordinates (× 10^4) for **7**

Atom	*x*	*y*	*z*
Bi(1)	6528.0(6)	1037.6(6)	5474.2(5)
Bi(2)	4183.9(7)	1405.9(7)	6715.4(6)
Br(1)	8605(2)	866(2)	6083(2)
Br(2)	6333(2)	899(2)	3601(2)
Br(3)	6703(2)	1189(2)	7246(2)
Br(4)	4177(2)	1375(2)	4820.1(14)
Br(5)	4477(2)	3427(2)	6707(2)
Br(6)	4128(2)	1422(3)	8366(2)
P(1)	6736(4)	3096(4)	5394(4)
C(1)	7626(22)	3380(15)	4904(15)
C(2)	7925(22)	4540(19)	4872(18)
C(3)	5544(19)	3771(15)	4715(15)
C(4)	5048(19)	3560(20)	3713(15)
C(5)	7228(17)	3685(14)	6518(14)
C(6)	8365(22)	3424(17)	7145(17)
P(2)	2076(5)	1728(5)	5973(4)
C(7)	1535(20)	1917(20)	4745(17)
C(8)	1904(19)	2911(20)	4524(18)
C(9)	1330(22)	647(23)	6000(20)
C(10)	1507(25)	342(25)	7029(22)
C(11)	1830(20)	2839(18)	6554(19)
C(12)	658(20)	3124(20)	6183(18)

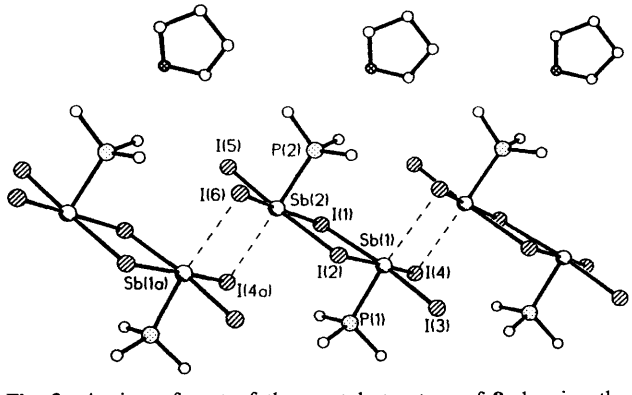

Fig. 2 A view of part of the crystal structure of **8** showing three $[Sb_2I_6(PMe_3)_2]$ dimer units and three thf molecules of crystallisation. The weaker bridging interactions between dimer units are indicated by dotted lines

Table 3 Selected bond lengths (Å) and angles (°) for **8***

Sb(1)–P(1)	2.633(6)	Sb(1)–I(3)	2.836(2)
Sb(1)–I(4)	2.970(2)	Sb(1)–I(2)	3.016(2)
Sb(1)–I(1)	3.225(2)	Sb(1)–I(6a)	3.698(2)
Sb(2)–P(2)	2.627(5)	Sb(2)–I(5)	2.847(2)
Sb(2)–I(6)	2.894(2)	Sb(2)–I(1)	3.092(2)
Sb(2)–I(2)	3.230(2)	Sb(2)–I(4b)	3.547(2)
I(4)–Sb(2a)	3.547(2)	I(6)–Sb(1b)	3.698(2)
P(1)–Sb(1)–I(3)	87.33(13)	P(1)–Sb(1)–I(4)	83.98(13)
I(3)–Sb(1)–I(4)	94.33(6)	P(1)–Sb(1)–I(2)	92.51(13)
I(3)–Sb(1)–I(2)	92.03(6)	I(4)–Sb(1)–I(2)	172.58(6)
P(1)–Sb(1)–I(1)	88.99(13)	I(3)–Sb(1)–I(1)	175.59(6)
I(4)–Sb(1)–I(1)	87.70(5)	I(2)–Sb(1)–I(1)	85.70(5)
P(1)–Sb(1)–I(6a)	174.72(13)	I(3)–Sb(1)–I(6a)	87.71(5)
I(4)–Sb(1)–I(6a)	94.58(5)	I(2)–Sb(1)–I(6a)	89.48(6)
I(1)–Sb(1)–I(6a)	96.05(5)	P(2)–Sb(2)–I(5)	86.74(12)
P(2)–Sb(2)–I(6)	86.28(13)	I(5)–Sb(2)–I(6)	94.87(6)
P(2)–Sb(2)–I(1)	90.86(13)	I(5)–Sb(2)–I(1)	92.54(6)
I(6)–Sb(2)–I(1)	171.89(6)	P(2)–Sb(2)–I(2)	91.49(12)
I(5)–Sb(2)–I(2)	176.43(6)	I(6)–Sb(2)–I(2)	88.10(5)
I(1)–Sb(2)–I(2)	84.39(5)	P(2)–Sb(2)–I(4b)	173.78(13)
I(5)–Sb(2)–I(4b)	89.87(5)	I(6)–Sb(2)–I(4b)	99.22(6)
I(1)–Sb(2)–I(4b)	84.08(5)	I(2)–Sb(2)–I(4b)	91.61(5)
Sb(2)–I(1)–Sb(1)	94.15(5)	Sb(1)–I(2)–Sb(2)	95.51(5)
Sb(1)–I(4)–Sb(2a)	83.93(5)	Sb(2)–I(6)–Sb(1b)	82.26(5)

* Symmetry transformations used to generate equivalent atoms: a, $x + 1, y, z$; b, $x - 1, y, z$.

Table 4 Atomic coordinates ($\times 10^4$) for **8**

Atom	x	y	z
Sb(1)	6640(2)	4364.2(10)	6505.4(5)
Sb(2)	1330(2)	2878.7(10)	5991.4(5)
I(1)	4624(2)	2172.5(10)	6596.5(5)
I(2)	3320(2)	5098.0(10)	5975.1(5)
I(3)	8202(2)	6364.0(11)	6461.9(6)
I(4)	9613(2)	3451.1(11)	7090.1(5)
I(5)	−215(2)	861.6(11)	6009.7(6)
I(6)	−1438(2)	3769.8(11)	5376.6(5)
P(1)	5489(7)	4925(4)	7320(2)
C(1)	4861(38)	3815(18)	7665(8)
C(2)	3608(32)	5761(18)	7270(8)
C(3)	7171(31)	5601(17)	7675(7)
P(2)	2773(7)	2281(4)	5223(2)
C(4)	1298(29)	1612(21)	4814(10)
C(5)	4574(35)	1399(18)	5349(9)
C(6)	3673(29)	3391(16)	4911(7)
O	4992(23)	1293(15)	4204(6)
C(7)	4561(31)	913(19)	3746(8)
C(8)	6129(41)	1026(25)	3460(9)
C(9)	7316(38)	1780(18)	3734(11)
C(10)	6746(36)	1642(21)	4229(12)

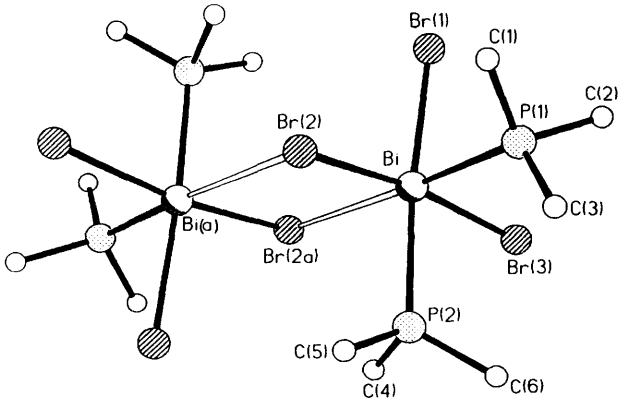

Fig. 3 A view of the molecular structure of **2**

lengths: Sb(1)–I(1) 3.225(2), Sb(2)–I(1) 3.092(2), difference (Δ) = 0.133 Å, and Sb(1)–I(2) 3.016(2), Sb(2)–I(2) 3.230(2), Δ = 0.214 Å.

Within the dimer, iodines I(3) and I(5) may be described as terminal and these have the shortest Sb–I lengths [Sb(1)–I(3) 2.836(2) and Sb(2)–I(5) 2.847(2) Å], but the remaining iodines I(4) and I(6) form weak bridging interactions to adjacent dimer units and are thus slightly longer [Sb(1)–I(4) 2.970(2) and Sb(2)–I(6) 2.894(2) Å]. These weak interactions are defined by Sb(2)–I(4b) 3.547(2) and Sb(1b)–I(6) 3.698(2) Å, the relevant bond length differences, Δ, to the two antimony centres being 0.804 Å for I(6) and 0.577 Å for I(4), thus characterising these interactions as highly asymmetric (and hence weak) consistent with the above description of the overall structure as a polymer of dimers or, to be more precise, a weakly bound polymer of strongly bound dimers. These long Sb···I interactions are *trans* to the Sb–P bonds (the *trans* influence evident in **7** is found here also) such that the overall co-ordination geometry around the antimony centres is octahedral if these interactions are considered. Furthermore, the bond angles are all within 10° of idealised values implying that the Sb^{III} lone pair has no appreciable angular stereochemical activity.

The Sb–P bond lengths [Sb(1)–P(1) 2.633(6) and Sb(2)–P(2) 2.627(5) Å] are similar to those found in **4** [2.6658(14) and 2.6437(14) Å] but longer than those observed in **5** [2.596(4) Å] and **6** [2.594(6) Å], the shorter values for the latter two complexes probably reflecting the lower co-ordination numbers (four) of the antimony centres. The fact that thf occurs in crystals of **8** but unco-ordinated to the antimony, implies that PMe_3 is probably a better ligand than thf toward the SbI_3 molecule.

The structure of **8** is quite similar to that of the previously reported complex $[BiI_3(hmpa)]$ **9** [hmpa = hexamethylphosphoramide, $OP(NMe_2)_3$].[14] In complex **9**, the structure may also be described as a polymer of dimers in which two bismuth atoms are linked by a pair of symmetrically bridging iodines with the dimers associated through weaker pairs of asymmetrically bridging iodines (each bismuth is additionally bonded to a terminal iodine and one hmpa ligand). In this case, the difference between the symmetric and asymmetric pairs of iodines is not so marked as it is in **8**, but the major difference between the two structures is that in **8** the two PMe_3 ligands are bonded perpendicular to the plane of the symmetric $Sb_2(\mu\text{-}I)_2$ unit whereas in **9**, the hmpa ligands lie in the symmetric $Bi_2(\mu\text{-}I)_2$ plane; this is evident from a comparison of Fig. 2 and of Fig. 1 in ref. 14. If the asymmetric bridging interactions in **8**, I(4) and I(6), became symmetric and the symmetric bridging interactions, I(1) and I(2), became asymmetric, the structure of **8** would be of the same type as that of **9**. This difference in structure is an indication that the *trans* influence of hmpa is considerably less than that of PMe_3 in these types of compound.

We now turn to complexes of the general formula $[EX_3(L)_2]$, some general structural types for which were discussed in ref. 14. The reaction between $BiBr_3$ and PMe_3 using PMe_3 as a reaction medium afforded, after work-up, yellow crystals of the complex $[Bi_2Br_6(PMe_3)_4]$ **2** as described in ref. 6. The structure was established by X-ray crystallography the results of which are shown in Fig. 3; selected bond lengths and angles are given in Table 5 and atomic positional parameters are presented in Table 6. The structure of **2** is best described as a centrosymmetric (crystallographic) edge-shared, bioctahedral dimer in which each of the two bismuth centres is bonded to two PMe_3 ligands and four bromines; there are no short intermolecular contacts. Three of the Bi–Br distances are quite similar [Bi–Br(1) 2.9164(13), Bi–Br(2) 2.8750(11) and Bi–Br(3) 2.7749(11) Å] but the fourth [Bi–Br(2a) 3.4034(12) Å] is significantly longer and as such, the bromines Br(2) and Br(2a) which bridge between the two bismuth centres do so quite asymmetrically (Δ = 0.528 Å). Furthermore, it is interesting that the Bi–Br(2) distance is shorter than the Bi–Br(1) distance

Table 5 Selected bond lengths (Å) and angles (°) for **2***

Bi–P(1)	2.716(3)	Bi–Br(3)	2.7749(11)
Bi–P(2)	2.865(3)	Bi–Br(2)	2.8750(11)
Bi–Br(1)	2.9164(13)	Bi–Br(2a)	3.4034(12)
P(1)–Bi–Br(3)	89.37(6)	P(1)–Bi–P(2)	92.41(8)
Br(3)–Bi–P(2)	82.23(6)	P(1)–Bi–Br(2)	86.54(6)
Br(3)–Bi–Br(2)	167.41(4)	P(2)–Bi–Br(2)	86.05(6)
P(1)–Bi–Br(1)	80.37(7)	Br(3)–Bi–Br(1)	97.32(4)
P(2)–Bi–Br(1)	172.77(6)	Br(2)–Bi–Br(1)	93.72(4)
P(1)–Bi–Br(2a)	176.17(6)	Br(3)–Bi–Br(2a)	94.46(3)
P(2)–Bi–Br(2a)	88.41(6)	Br(2)–Bi–Br(2a)	89.78(3)
Br(1)–Bi–Br(2a)	98.82(3)	Bi–Br(2)–Bi(a)	90.22(3)

* Symmetry transformations used to generate equivalent atoms: a, $-x + 1, -y + 1, -z + 1$.

Table 6 Atomic coordinates ($\times 10^4$) for **2**

Atom	*x*	*y*	*z*
Bi	5213.0(4)	6750.7(3)	4571.7(2)
Br(1)	7654(2)	6408.3(11)	3407.6(7)
Br(2)	3034.3(14)	4968.9(9)	3930.4(6)
Br(3)	6659(2)	8667.8(9)	5284.9(7)
P(1)	3730(4)	8000(2)	3322(2)
C(1)	3371(18)	7176(11)	2417(6)
C(2)	5107(16)	9137(9)	3106(7)
C(3)	1721(16)	8636(10)	3442(8)
P(2)	2592(3)	7269(2)	5565(2)
C(4)	3589(18)	6994(13)	6577(7)
C(5)	720(15)	6407(11)	5457(8)
C(6)	1784(17)	8682(10)	5627(9)

even though the former bond is part of the bridging interaction and the latter is terminal. This undoubtedly reflects the strong *trans* influence of the PMe_3 ligand P(2), a feature which we have encountered previously in **8** and, for PEt_3, in **7**; the other phosphine, P(1), is *trans* to the long Bi–Br(2a) bond. The Bi–P bond lengths [Bi–P(1) 2.716(3) and Bi–P(2) 2.865(3) Å] are similar to those found in **1**, **3** and **7** (see above) and the co-ordination geometry around the bismuth centres is close to regular octahedral as seen in the previous structures.

It is informative to compare the structure of **2** with other examples of edge-shared, bioctahedral compounds of the general formula $[E_2X_6(L)_4]$ where E is an element centre in the +3 oxidation state, X is halide and L is a monodentate, two-electron donor ligand. In the chemistry of p-block element(III) compounds, this type of structure is rare, the only other examples being **3** and the complex $[Bi_2I_6(OPPh_3)_4]$ **10**,[15] and all three structures have a centrosymmetric structure as shown in **A**. We note, though without a satisfactory explanation, that analogous In^{III} and Tl^{III} complexes are invariably monomeric, *i.e.* $[EX_3(L)_2]$ (E = In or Tl).[16] There are, however, a large number of transition metal complexes with this formula for which some interesting structural differences are apparent. In fact, for monodentate L, two isomers different from **A** are commonly found.

Examples of isomers where all ligands are in what we may describe as the equatorial plane of the molecule, *i.e.* the $E_2(\mu\text{-}X)_2$ plane, type **B**, are $[Zr_2Cl_6(L)_4]$ (L = PBu^n_3,[17] PEt_3[18] or PMe_2Ph[18]), $[Zr_2I_6(L)_4]$ (L = PMe_3[19] or PMe_2Ph[19]), $[Hf_2Cl_6(PEt_3)_4]$,[20] and $[Hf_2X_6(PMe_2Ph)_4]$ (X = Cl[21] or I[19]), whereas examples of the more common isomer **C**, where two ligands are in equatorial sites and two are in axial sites, are $[V_2Cl_6(PMe_3)_4]$,[22] $[Ta_2Cl_6(PMe_3)_4]$,[23] $[Cr_2Cl_6(L)_4]$ (L = PMe_3[24] or PEt_3[24]), $[W_2Cl_6(L)_4]$ (L = PMe_3[25] or PMe_2Ph[26]), $[Ru_2Cl_6(PBu^n_3)_4]$[27] and $[Rh_2Cl_6(L)_4]$ (L = PEt_3[28] or PBu^n_3[28]). It is evident that the type **B** form is found for elements from Group 4 (d^1 metal centres) whereas complexes with elements from Groups 5 to 9 (d^2 to d^6 metal

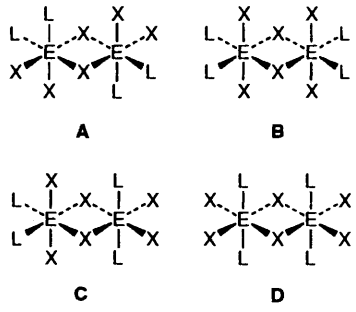

centres) adopt a type **C** structure (although there are apparently no examples of d^4–d^4 complexes with monodentate L). Exceptions to this general rule are, however, found for the thf complex $[Ti_2Cl_6(thf)_4]$, which has a type **C** structure, and the related vanadium complex $[V_2Cl_6(thf)_4]$ which has a type **A** structure.[29] A further structural type is observed in the ytterbium thf complex $[Yb_2Cl_6(thf)_4]$[30] which has a different structure of type **D** in which all ligands are axial; this is uncommon for monodentate L, but is frequently encountered in transition-metal systems with bidentate phosphines of the form $R_2PCH_2PR_2$ which bridge between the metal centres. Many other complexes are also known with a range of bidentate phosphines which we will not comment on in detail here although we will return to a couple of specific examples later.

The factors affecting which type of structure is adopted have not been well understood, as commented upon by Cotton *et al.*,[18] but a number of recent studies have addressed this matter in more detail. Cotton *et al.*,[31] have recently described some unusual (for transition metal complexes) isomers of some ditungsten/dimolybdenum complexes, and Poli and Gordon[32] have commented in detail upon the relationship between the precise structures of a series of dimolybdenum complexes and the nature of the M–M interaction. In a subsequent study, however, Poli and Torralba[33] have considered, from a theoretical standpoint, the factors affecting the adoption of a particular geometry or isomeric form, some aspects of which are relevant here. We will not reiterate all the details of their analysis, and clearly any features relevant to metal–metal bonding in the d-block compounds, where the electron count per metal ranges from d^1 to d^6, are not relevant to bismuth(III) and antimony(III) complexes in which the metal electron count is $[d^{10}]s^2$; with this latter electron configuration, metal–metal bonding is unlikely to be significant, although closed-shell M–M interactions involving the heavier elements should not be ruled out, *viz.* the structural chemistry of many Au^I and Tl^I compounds. The analysis of Poli and Torralba indicates that, at least for structures **B**, **C** and **D** which they considered, type **C** is the lowest energy form in terms of the steric interactions between the ligands, L. Thus in **B**, there are unfavourable interactions between the two pairs of *cis*-related ligands per metal centre in the equatorial plane, whereas in **D**, steric interactions between pairs of *syn*-axial ligands are maximised. Isomer **C**, therefore, represents a compromise between these two forms, although type **D** structures are expected for certain bridging diphosphines or small monodentate ligands such as thf as in $[Yb_2Cl_6(thf)_4]$. The reason for the preference for the sterically less preferred type **B** structure for the d^1–d^1 complexes is traced to an electronic factor involving favourable M–X $d\pi$–$p\pi$ interactions for this particular electron count.

In the absence of any likely M–M or M–X $d\pi$–$p\pi$ bonding considerations, we are then left with a consideration of why the bismuth complexes **2**, **3** and **10** adopt the type **A** structure rather than the sterically preferred type **C** structure. The fact that the type **A** structure places both ligands per metal centre *cis* to each other (as does **B**) is suggestive of the fact that the structure is

controlled more by electronic effects (as for type **B** in d^1–d^1 compounds) than by steric effects although we must be careful here. There is a considerable range in the M–P bond lengths of the various compounds, these being about 2.7–2.8 Å for the Bi and Hf compounds decreasing to 2.3 Å for the Ru and Rh compounds; steric effects will be much more important in the latter. However, we must also note that in the bismuth compounds, the bonding situation is quite different from that in the d-block element compounds. In the latter, the phosphines (or ligands in general) interact with the metal based d orbitals, whereas in the bismuth complexes, the d-orbital manifold is filled and essentially core in nature, and it is the vacant Bi–X σ* orbitals (X = halide) which are the likely acceptor orbitals through which the ligands interact.[12] On the basis of this model, we expect that the ligands L will generally bond *trans* to a halide rather than *trans* to each other since the halide is the more electronegative group and therefore has the lower energy σ* orbital.[12] This accounts for the absence of type **C** and **D** structures though not for the absence of type **B**; we will return to this matter shortly.

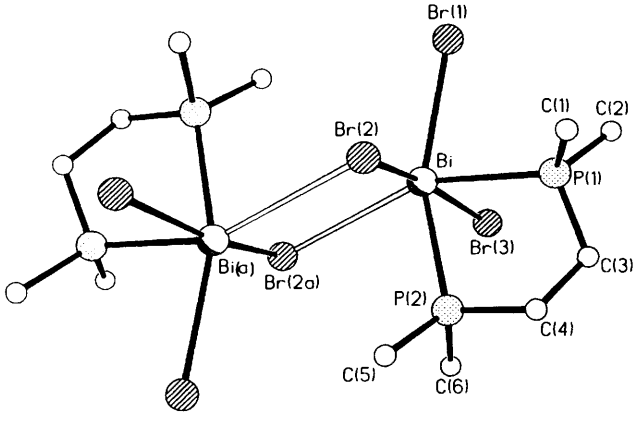

Fig. 4 A view of the molecular structure of **11**

Table 7 Selected bond lengths (Å) and angles (°) for **11***

Bi–P(1)	2.678(8)	Bi–Br(3)	2.788(3)
Bi–P(2)	2.791(7)	Bi–Br(2)	2.887(3)
Bi–Br(1)	2.992(3)	Bi–Br(2a)	3.345(3)
P(1)–Bi–Br(3)	81.8(2)	P(1)–Bi–P(2)	76.3(2)
Br(3)–Bi–P(2)	84.5(2)	P(1)–Bi–Br(2)	89.8(2)
Br(3)–Bi–Br(2)	165.99(10)	P(2)–Bi–Br(2)	82.6(2)
P(1)–Bi–Br(1)	80.1(2)	Br(3)–Bi–Br(1)	98.19(10)
P(2)–Bi–Br(1)	155.6(2)	Br(2)–Bi–Br(1)	91.32(9)
P(1)–Bi–Br(2a)	154.4(2)	Br(3)–Bi–Br(2a)	93.30(9)
P(2)–Bi–Br(2a)	78.3(2)	Br(2)–Bi–Br(2a)	89.48(8)
Br(1)–Bi–Br(2a)	125.49(9)	Bi–Br(2)–Bi(a)	90.52(8)

* Symmetry transformations used to generate equivalent atoms: a, $-x + 1, -y + 1, -z + 1$.

Table 8 Atomic coordinates (× 10^4) for **11**

Atom	*x*	*y*	*z*
Bi	5002.7(13)	3485.7(9)	5816.7(6)
Br(1)	5424(4)	3965(3)	7575(2)
Br(2)	2510(4)	5371(2)	5628(2)
Br(3)	6783(4)	1374(3)	5780(2)
P(1)	2388(11)	2156(7)	6382(4)
P(2)	3262(10)	2676(7)	4433(4)
C(1)	545(46)	2971(30)	6716(19)
C(2)	3122(52)	1200(30)	7207(17)
C(3)	1683(43)	1239(24)	5587(17)
C(4)	1322(39)	1902(28)	4775(15)
C(5)	2402(42)	3699(25)	3671(17)
C(6)	4614(41)	1718(28)	3859(20)

Further examples of edge-shared, bioctahedral complexes were obtained from the reaction between $BiBr_3$ or $SbBr_3$ and dmpe. The reaction between $BiBr_3$ and one equivalent of dmpe afforded pale yellow-green crystals of the complex $[Bi_2Br_6(dmpe)_2]$ **11**, the structure of which was established by X-ray crystallography. The results are shown in Fig. 4 with selected bond lengths and angles given in Table 7 and atomic positional parameters presented in Table 8. The structure is also of type **A** as found for **2** with similarly asymmetric bridging bromines Br(2) and Br(2a) [Bi–Br(2) 2.887(3), Bi–Br(2a) 3.345(3), Δ = 0.458 Å] (the same atom numbering scheme has been adopted for **2** and **11**). Also as for **2**, the Bi–Br(3) distance is the shortest [Bi–Br(3) 2.788(3) Å] with that to Br(1) [Bi–Br(1) 2.992(3) Å] being longer than that to Br(2) and reflecting the *trans* influence of the phosphine P(2). Indeed, the crystal and molecular structures of **2** and **11** are similar in all respects, the major difference being the P–Bi–P angle [92.41(8)° for **2** and 76.3(2)° in **11**] and the opposite Br(1)–Bi–Br(2a) angle [98.82(3)° for **2** and 125.49(9)° for **11**].

The analogous reaction between $SbBr_3$ and dmpe also afforded a crystalline compound but this was shown by X-ray crystallography to be a mixture of two different polymorphs of empirical formula $[SbBr_3(dmpe)]$. The first of these, $[Sb_2Br_6(dmpe)_2]$ **12** was found to be isomorphous with **11**; a view of **12** (numbering scheme as for **2** and **11**) is shown in Fig. 5, selected bond lengths and angles are given in Table 9 and atomic positional parameters are presented in Table 10. The other polymorph, which may be described as a linear tetramer $[Sb_4Br_{12}(dmpe)_4]$ **13** is shown in Fig. 6 with selected bond lengths and angles given in Table 11 and atomic positional parameters presented in Table 12.

Looking first at **12**, the major difference between this complex and **11** is the asymmetry of the bromine bridges. In **11** the relevant distances are given above for which the difference (Δ) is 0.458 Å, whereas for **12** the corresponding distances are

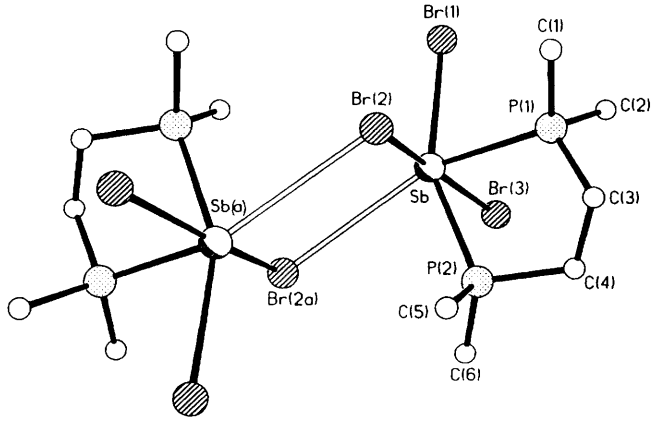

Fig. 5 A view of the molecular structure of **12**

Table 9 Selected bond lengths (Å) and angles (°) for **12***

Sb–P(1)	2.575(2)	Sb–P(2)	2.659(3)
Sb–Br(3)	2.6954(12)	Sb–Br(2)	2.8280(12)
Sb–Br(1)	3.0033(13)	Sb–Br(2a)	3.5954(12)
P(1)–Sb–P(2)	79.18(8)	P(1)–Sb–Br(3)	86.70(6)
P(2)–Sb–Br(3)	80.28(6)	P(1)–Sb–Br(2)	84.27(6)
P(2)–Sb–Br(2)	87.20(7)	Br(3)–Sb–Br(2)	165.75(4)
P(1)–Sb–Br(1)	78.57(6)	P(2)–Sb–Br(1)	155.65(6)
Br(3)–Sb–Br(1)	88.68(3)	Br(2)–Sb–Br(1)	100.28(4)
P(1)–Sb–Br(2a)	147.49(7)	P(2)–Sb–Br(2a)	73.50(6)
Br(3)–Sb–Br(2a)	105.36(3)	Br(2)–Sb–Br(2a)	77.22(3)
Br(1)–Sb–Br(2a)	130.66(3)	Sb–Br(2)–Sb(a)	102.78(3)

* Symmetry transformations used to generate equivalent atoms: a, $-x, -y + 1, -z + 2$.

Table 10 Atomic coordinates ($\times 10^4$) for **12**

Atom	*x*	*y*	*z*
Sb	263.1(8)	3 678.0(5)	8 785.5(4)
Br(1)	− 55.0(14)	4 376.1(9)	6 969.2(6)
Br(2)	2 346.1(13)	5 485.6(8)	9 524.9(6)
Br(3)	−1 065.9(13)	1 648.4(8)	8 294.2(6)
P(1)	3 371(3)	3 009(2)	8 335(2)
P(2)	1 518(3)	2 468(2)	10 120(2)
C(1)	4 841(13)	4 108(9)	8 036(7)
C(2)	3 092(14)	2 048(8)	7 461(6)
C(3)	4 587(12)	2 281(8)	9 233(6)
C(4)	3 274(13)	1 576(9)	9 729(6)
C(5)	2 647(13)	3 226(9)	10 998(6)
C(6)	−111(14)	1 533(9)	10 544(6)

Table 11 Selected bond lengths (Å) and angles (°) for **13***

Sb(1)–P(1)	2.584(3)	Sb(1)–P(2)	2.662(3)
Sb(1)–Br(3)	2.723(2)	Sb(1)–Br(2)	2.787(2)
Sb(1)–Br(1)	3.000(2)	Sb(1)–Br(2a)	3.493(2)
Br(1)–Sb(2)	3.334(2)	Br(2)–Sb(1a)	3.493(2)
Sb(2)–P(4)	2.498(6)	Sb(2)–Br(5)	2.648(3)
Sb(2)–P(3A)	2.656(4)	Sb(2)–P(3)	2.656(4)
Sb(2)–P(4A)	2.731(7)	Sb(2)–Br(4A)	2.741(3)
Sb(2)–Br(5A)	2.762(3)	Sb(2)–Br(6)	2.879(2)
Sb(2)–Br(4)	2.910(3)	Sb(2)–Br(6A)	3.126(3)
P(1)–Sb(1)–P(2)	79.08(9)	P(1)–Sb(1)–Br(3)	85.76(8)
P(2)–Sb(1)–Br(3)	85.55(7)	P(1)–Sb(1)–Br(2)	85.08(8)
P(2)–Sb(1)–Br(2)	84.63(7)	Br(3)–Sb(1)–Br(2)	167.68(4)
P(1)–Sb(1)–Br(1)	79.60(8)	P(2)–Sb(1)–Br(1)	158.57(7)
Br(3)–Sb(1)–Br(1)	95.07(5)	Br(2)–Sb(1)–Br(1)	91.37(4)
P(1)–Sb(1)–Br(2a)	153.44(8)	P(2)–Sb(1)–Br(2a)	75.87(7)
Br(3)–Sb(1)–Br(2a)	100.82(4)	Br(2)–Sb(1)–Br(2a)	83.97(4)
Br(1)–Sb(1)–Br(2a)	124.74(4)	Sb(1)–Br(1)–Sb(2)	157.32(5)
Sb(1)–Br(2)–Sb(1a)	96.03(4)	P(4)–Sb(2)–Br(5)	95.4(3)
P(4)–Sb(2)–P(3)	76.1(2)	Br(5)–Sb(2)–P(3)	77.06(12)
P(3A)–Sb(2)–P(4A)	82.4(2)	P(3A)–Sb(2)–Br(4A)	81.98(11)
P(4A)–Sb(2)–Br(4A)	86.6(2)	P(3A)–Sb(2)–Br(5A)	91.32(12)
P(4A)–Sb(2)–Br(5A)	77.7(2)	Br(4A)–Sb(2)–Br(5A)	163.63(10)
P(4)–Sb(2)–Br(6)	82.0(2)	Br(5)–Sb(2)–Br(6)	88.95(10)
P(3)–Sb(2)–Br(6)	152.62(11)	P(4)–Sb(2)–Br(4)	81.8(3)
Br(5)–Sb(2)–Br(4)	161.89(10)	P(3)–Sb(2)–Br(4)	84.91(11)
Br(6)–Sb(2)–Br(4)	108.22(9)	P(3A)–Sb(2)–Br(6A)	154.29(10)
P(4A)–Sb(2)–Br(6A)	72.83(14)	Br(4A)–Sb(2)–Br(6A)	89.50(10)
Br(5A)–Sb(2)–Br(6A)	90.21(10)	P(4)–Sb(2)–Br(1)	149.3(2)
Br(5)–Sb(2)–Br(1)	87.73(8)	P(3A)–Sb(2)–Br(1)	74.85(9)
P(3)–Sb(2)–Br(1)	74.85(9)	P(4A)–Sb(2)–Br(1)	156.13(13)
Br(4A)–Sb(2)–Br(1)	97.29(8)	Br(5A)–Sb(2)–Br(1)	95.32(8)
Br(6)–Sb(2)–Br(1)	128.65(6)	Br(4)–Sb(2)–Br(1)	85.90(8)
Br(6A)–Sb(2)–Br(1)	130.52(6)		

* Symmetry transformations used to generate equivalent atoms: a, $-x+1, -y, -z+2$.

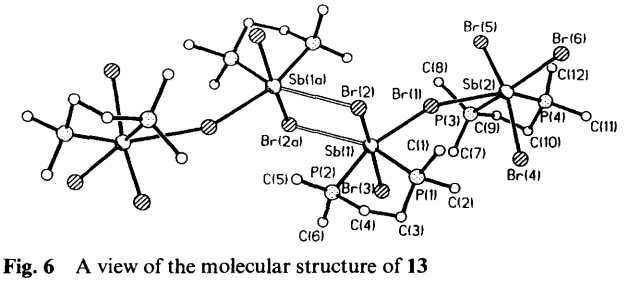

Fig. 6 A view of the molecular structure of **13**

Sb–Br(2) 2.8280(12) and Sb–Br(2a) 3.5954(12) with Δ 0.767 Å. This feature is, in fact, quite general in that, in isomorphous pairs of antimony and bismuth structures, bridge asymmetry is greatest for antimony and least for bismuth; this feature is also encountered in the structures of SbI_3 and BiI_3 and is discussed in more detail in refs. 10 and 12.

The structure of **13** is rather different and was plagued by serious disorder problems, but the gross molecular geometry is clear and may be described as a centrosymmetric (crystallographic) tetramer. The central part of this tetramer is similar to the dimer unit present in **12** in having a type **A** isomeric structure with highly asymmetric Sb–Br–Sb bridges; Sb(1)–Br(2) 2.787(2), Sb(1)–Br(2a) 3.493(2), Δ = 0.706 Å, the value of Δ being much closer to **12** than to **11** providing independent confirmation of the trend towards greater asymmetry for antimony. The central dimer unit is then linked through Br(1) and Br(1a) to two $SbBr_3$(dmpe) groups, Br(1)–Sb(2) 3.334(2), Br(1)–Sb(1) 3.000(2) Å, the bromine atom Br(1) being close to linear, Sb(1)–Br(1)–Sb(2) 157.32(5)°. The angles around the antimony centres show reduced P–Sb–P and enlarged, opposite Br–Sb–Br angles as seen in **12** (and **11**, and also **4**[7,34]).

Compounds **11** and **12** (and the central unit of **13**) may be compared with the ditungsten complex $[W_2Cl_6(dmpe)_2]$ **14** which has been described recently by Cotton *et al.*[31] Complex **14** has the same type **A** structure as the antimony and bismuth complexes (which is unusual for a d-block complex as mentioned above, and as commented upon by Cotton), but a major difference between the p- and d-block element structures lies in the degree of symmetry of the halide bridges. In **11**–**13** the halide bridges are highly asymmetric as discussed above, whereas in **14**, the bridging atoms are much more symmetrically bonded: W–Cl 2.381(4) and 2.398(4), Δ = 0.017 Å. Indeed, symmetrical halide bridges in the transition metal(III) dimers are a quite general feature, a list of relevant distances being given in ref. 33, even when, in the type **C** structure, the groups *trans* to the bridging halide are not the same which, in turn, implies a much smaller phosphine *trans* influence in the d- *vs.* p-block complexes.

These structural differences undoubtedly reflect differences in the nature of the bonding orbitals present. Thus, in the d-block element compounds, the metal-based electrons lie in the d-orbital manifold and while they may or may not interact through the formation of M–M and M–X dπ–pπ bonds, they exert no (or little) stereochemical influence in terms of the asymmetrical lengthening of certain bonds such as those in the $M_2(\mu\text{-}X)_2$ unit. In the p-block element(III) complexes with a $[d^{10}]s^2$ electron configuration, however, the situation is rather different. The d orbitals, being now filled, are essentially a spherically symmetric core sub-shell which will have little effect on the co-ordination geometry, but the stereochemical effect of the s^2 pair is all important. This pair is formally a lone or non-bonding pair and its stereochemical activity or otherwise is a very important aspect of structural p-block chemistry. In the case of complexes **11**–**13**, we may view the bridge asymmetry as the result of lone-pair localisation along the vector of the long E–(μ-X) bond *trans* to a phosphine (the *trans* influence of the phosphine may indeed be seen in terms of its effect in localising a lone pair). In the event that this were taken to an extreme, whereby complete dissociation occurred and the complexes existed as $[EX_3(L)_2]$ monomers, the resulting square-based pyramidal geometry would be that expected from valence shell electron pair repulsion arguments for a five-co-ordinate, six-electron pair species. We may therefore view these complexes as examples where the lone pair is partially active, the less so for bismuth, and in which the stereochemical activity is manifest largely as a lengthening of certain bonds although some angular distortions are also present in **11**–**13**.

As a general point, if we consider the case of an octahedral p-block complex with O_h symmetry for the electron counts relevant here, distortions associated with the onset of lone-pair stereochemical activity are likely to be of T_{1u} symmetry which may occur either as a coupled lengthening and shortening of two *trans* bonds (a C_{4v} distortion without angle changes), an opening of an angle between a pair of *cis* groups or ligands (a C_{2v} distortion with localisation of the lone pair along an edge of the octahedron), or as an opening of the angles between a set of three facial ligands (a C_{3v} distortion with localisation of the lone pair in one face of the octahedron); bond lengths adjacent to the

Table 12 Atomic coordinates (× 10^4) for **13**

Atom	x	y	z	Atom	x	y	z
Sb(1)	4794.2(9)	83.2(3)	8341.1(5)	Br(6)	6782(3)	2820.8(9)	6014(2)
Br(1)	4713(2)	1104.7(5)	7599.0(8)	Br(4A)	5020(4)	1424.8(12)	4487(2)
Br(2)	7533.4(14)	318.3(4)	9939.0(7)	Br(5A)	3152(4)	2683.3(12)	7057(2)
Br(3)	2648(2)	−288.3(5)	6705.3(8)	Br(6A)	7404(3)	2717.2(9)	5604(2)
P(1)	7402(4)	44.6(11)	7430(2)	P(3)	1216(4)	1553(2)	5552(2)
P(2)	5949(4)	−825.5(10)	8712(2)	P(4)	2927(8)	2344(4)	4386(5)
C(1)	9244(15)	459(5)	7868(9)	C(7)	1196(20)	907(6)	5255(10)
C(2)	6556(28)	267(10)	6113(15)	C(8)	−32(55)	1718(16)	6598(28)
C(3)	7979(31)	−573(8)	7283(18)	C(9)	−86(18)	1861(8)	4486(11)
C(4)	8150(34)	−815(9)	8268(20)	C(10)	1232(26)	1908(8)	3766(14)
C(5)	6848(21)	−989(5)	9954(10)	C(11)	4511(38)	2450(9)	3591(16)
C(6)	4498(42)	−1239(10)	8044(28)	C(12)	1832(38)	2913(8)	4506(19)
C(1A)	9244(15)	459(5)	7868(9)	P(3A)	1216(4)	1553(2)	5552(2)
C(2A)	6903(29)	23(10)	6215(16)	P(4A)	2738(8)	2629(4)	4602(5)
C(3A)	8709(32)	−551(9)	7882(21)	C(7A)	1196(20)	907(6)	5255(10)
C(4A)	7466(42)	−986(10)	7941(21)	C(8A)	−219(42)	1499(14)	6391(22)
C(5A)	6848(21)	−989(5)	9954(10)	C(9A)	−86(18)	1861(8)	4486(11)
C(6A)	4010(48)	−1320(13)	8421(30)	C(10A)	312(29)	2507(10)	4545(17)
Sb(2)	4443.6(10)	1989.6(3)	5975.9(5)	C(11A)	3249(43)	2516(9)	3415(18)
Br(4)	5523(4)	1254.6(12)	4744(2)	C(12A)	3066(28)	3252(8)	4814(16)
Br(5)	2513(4)	2491.4(11)	6985(2)				

lone pair may or may not be lengthened as well in the C_{2v} and C_{3v} distortions. Some of these matters have been discussed in more detail for Group 15 element(III) halogenoanions by Wheeler and Kumar[35] and by Sheldrick and Horn.[36] Additional structural studies on anionic phosphine complexes of antimony and bismuth are described in the following paper where matters affecting lone-pair stereochemical activity in terms of such angular distortions, specifically C_{2v} distortions, are addressed and discussed further.[34]

Returning finally to the origin of the preference for the type **A** structure in the antimony and bismuth $[E_2X_6(L)_4]$ complexes, the presence of phosphines *trans* to each other is unlikely, as discussed above, since the σ*-orbital model predicts that any ligand or Lewis base will tend to bond *trans* to a more electronegative group. In these examples, X is probably more electronegative than L, it will therefore be the E–X rather than the E–L σ* orbitals which are lowest in energy and hence the primary acceptor orbitals. This accounts for the absence of the type **C** and **D** structures but not for the absence of type **B**. An explanation of this latter point is more problematical. In the type **B** structure all phosphines would be *trans* to a bridging halide which, in view of the aforementioned large *trans* influence of the phosphines, would tend to weaken all Bi–$Br_{bridging}$ bonds. In the extreme, this might lead to a structure best described as two $[EX_2(L)_2]^+$ cations loosely associated with two X^- anions, as illustrated in **E**, and with a strong resemblance to the structure of **4**.[7,34] One possible reason for this structure not being found may then be the resulting mutual repulsion of the two Bi lone pairs localised along the Bi–Bi vector, which would be a consequence of this description as discussed for **4**.[7,34] Some simple quantitative calculations would be useful on a number of model structures in order to obtain a more quantitative insight into these various factors.

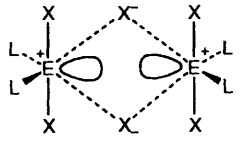

E

Experimental

General Procedures.—All experiments were performed under an atmosphere of dry, oxygen-free dinitrogen using standard Schlenk techniques. All solvents were dried and distilled over appropriate drying agents immediately prior to use. Microanalytical data were obtained at the University of Newcastle.

Antimony and bismuth trihalides (>99%) and PEt_3 and dmpe were procured commercially and used without further purification; PMe_3 was prepared by published methods. Compound **2** was prepared as described in ref. 6.

Preparations.—$[Bi_4Br_{12}(PEt_3)_4]$ **7**. A sample of $BiBr_3$ (0.254 g, 0.566 mmol) was dissolved in thf (10 cm^3) and stirred. To this two equivalents of PEt_3 (0.17 cm^3, 1.132 mmol) was added dropwise with constant stirring which caused an immediate colour change to a yellowish green. The resulting solution was allowed to stir for 1 h after which time the solvent volume was reduced by vacuum to about 5 cm^3 and hexane (15 cm^3) was added as an overlayer. Solvent diffusion over a period of a few weeks at room temperature afforded a homogeneous crop of yellowish green crystals of **7** (0.142 g, 44%), one of which was used for X-ray diffraction (Found: C, 15.05; H, 3.00. $C_6H_{15}BiBr_3P$ requires C, 12.70; H, 2.65%). The higher than predicted amounts of C and H are possibly due to excess phosphine sticking to the crystals or to the presence of some of a 2:1 phosphine complex.

$[Sb_2I_6(PMe_3)_2]$·thf **8**. A sample of SbI_3 (0.344 g, 0.685 mmol) was dissolved in thf (10 cm^3) which afforded a yellowish green solution. To this, a 0.5 mol dm^{-3} solution of PMe_3 in toluene (1.50 cm^3, 0.70 mmol) was added dropwise with constant stirring which caused the immediate precipitation of a yellow solid with a yellow solution remaining. All solvent was then removed by vacuum and the resulting yellow powder was washed in hexane. This yellow solid was found to be insoluble in MeCN, CH_2Cl_2 or $MeNO_2$, but was sparingly soluble in thf affording a yellow solution. This yellow solution (10 cm^3) was then transferred to a separate flask and hexane (25 cm^3) was then added as an overlayer. Solvent diffusion at −30 °C over a period of weeks afforded a small crop of yellow crystals of **8** in low yield, one of which was used for X-ray diffraction, the results of which revealed that **8** was a thf solvate (see text) (Found: C, 9.60; H, 2.10. $C_{10}H_{26}I_6OP_2Sb_2$ requires C, 9.75; H, 2.15%).

$[Bi_2Br_6(dmpe)_2]$ **11**. A sample of dmpe (0.13 cm^3, 0.749

Table 13 Crystallographic data[a]

Compound	**7**	**8**	**2**	**11**	**12**	**13**
Formula	$C_{24}H_{60}Bi_4Br_{12}P_4$	$C_{10}H_{26}I_6OP_2Sb_2$	$C_{12}H_{36}Bi_2Br_6P_4$	$C_{12}H_{32}Bi_2Br_6P_4$	$C_{12}H_{32}Br_6P_4Sb_2$	$C_{24}H_{64}Br_{12}P_8Sb_4$
M	2267.4	1229.2	1201.7	1197.7	1023.2	2046.4
Crystal size/mm	0.23 × 0.18 × 0.14	0.70 × 0.24 × 0.20	0.36 × 0.32 × 0.18	0.26 × 0.10 × 0.07	0.25 × 0.05 × 0.04	0.20 × 0.16 × 0.16
a/Å	14.138(10)	7.610(3)	7.9200(10)	7.502(2)	7.3050(11)	7.522(2)
b/Å	13.155(9)	12.846(4)	12.007(2)	11.579(4)	11.926(2)	27.524(9)
c/Å	16.156(12)	28.540(10)	16.608(2)	16.662(6)	15.964(3)	14.250(4)
β/°	114.41(5)	93.49(3)	96.61(2)	91.05(2)	95.72(2)	102.83(3)
U/Å^3	2736(3)	2785(2)	1568.8(4)	1447.2(8)	1383.8(4)	2877(2)
Z	2	4	2	2	2	2
D_c/g cm^{-3}	2.752	2.932	2.544	2.749	2.456	2.363
μ/mm^{-1}	21.720	8.705	19.046	20.647	10.845	10.434
F(000)	2032	2176	1088	1080	952	1904
2θ range/°	5–45	5–50	4–50	6–45	5–45	5–50
h, k, l ranges	−15 to 15, −13 to 14, −17 to 17	−9 to 9, −13 to 15, 0–33	−9 to 9, −13 to 14, −19 to 19	−8 to 8, −12 to 12, −17 to 17	−7 to 7, −12 to 12, −16 to 17	−8 to 8, −3 to 32, −16 to 16
No. of reflections measured	5389	5921	3686	2559	2635	5823
No. of unique reflections	3569	4869	2761	1872	1806	5039
No. with $F^2 > 2\sigma(F^2)$	2356	4065	2223	1469	1215	3582
Transmission factors	0.065, 0.022	0.008, 0.001	0.174, 0.039	0.659, 0.404	0.715, 0.525	0.253, 0.092
R_{int} (on F^2)	0.0941	0.0495	0.0426	0.1112	0.0500	0.0322
Weighting parameters a, b	0.1097, 0	0.1946, 50.3419	0.0696, 5.2256	0.0835, 65.3869	0.0205, 3.2478	0.0587, 37.9074
R [$F^2 > 2\sigma(F^2)$][b]	0.0610	0.0828	0.0397	0.0593	0.0296	0.0424
R' (all data)[b]	0.2066	0.3692	0.1119	0.2385	0.1016	0.1601
No. of parameters	200	190	115	109	113	317
Goodness of fit on F^2	1.049	1.109	1.079	1.365	1.011	1.116
Maximum, minimum in difference map/e Å^{-3}	3.326, −3.253	2.666, −1.739	2.190, −1.796	3.695, −1.828	0.757, −0.795	1.261, −1.875

[a] All crystals belong to the space group $P2_1/n$. [b] $R = \Sigma[|F_o| - |F_c|]/\Sigma|F_o|$, $R' = \{\Sigma[w(F_o^2 - F_c^2)^2]/\Sigma[w(F_o^2)^2]\}^{\frac{1}{2}}$.

mmol) was added dropwise to a stirred solution of $BiBr_3$ (0.336 g, 0.749 mmol) in thf (10 cm^3) (pale yellow) which resulted in the immediate precipitation of a cream solid. After stirring overnight, the solvent was removed by vacuum affording **11** as a cream solid which was then washed with hexane and dried (0.384 g, 86%) (Found: C, 12.25; H, 2.40. $C_6H_{16}BiBr_3P_2$ requires C, 12.05; H, 2.70%). Since **11** was not soluble in any common solvents, crystals suitable for X-ray diffraction were prepared in the following manner.

A solution of $BiBr_3$ (0.070 g, 0.157 mmol) in thf (5 cm^3) was prepared in a Schlenk flask of approximately 2 cm diameter, and an overlayer of fresh thf (5 cm^3) was then added. This was followed by the addition of a second overlayer of thf (5 cm^3) in which dmpe (0.03 cm^3, 0.156 mmol) had been dissolved. Finally, an overlayer of hexane (10 cm^3) was added and solvent diffusion over a period of several weeks afforded some pale yellow-green, needle-shaped crystals of **11** (0.071 g, 75%) (Found: C, 12.30; H, 2.55. $C_6H_{16}BiBr_3P_2$ requires C, 12.05; H, 2.70%).

$[Sb_2Br_6(dmpe)_2]$ **12/13**. Compound **12/13** was prepared in a similar manner to that described for **11** and was obtained also as a cream coloured solid (90%) which was insoluble in common solvents (Found: C, 14.30; H, 2.90. $C_6H_{16}Br_3P_2Sb$ requires C, 14.10; H, 3.15%).

Thin needle-like white crystals of **12/13** suitable for X-ray diffraction (two different polymorphs) were also prepared as for **11** (0.884 g, 90%) (Found: C, 14.40; H, 3.00. $C_6H_{16}Br_3P_2Sb$ requires C, 14.10; H, 3.15%).

X-Ray Crystallography.—Crystal data for all structures are given in Table 13 together with other information on data collection and structure determination.

Data collection and reduction. All measurements were made on a Stoe-Siemens diffractometer with graphite-monochromated Mo-Kα radiation (λ = 0.710 73 Å). Unit cell parameters were refined from 2θ values (20–25°) of 30–32 selected reflections measured on both sides of the beam to minimise systematic errors. All machine control calculations were performed with standard Stoe DIF4 software. Intensities were measured with ω/θ scans and on-line profile fitting,[37] except for compound **12**, for which the conventional background–peak–background method was used. Data were measured at 160(1) K [240(1) K for **2**] by use of a Cryostream cooler.[38] All the crystals belong to the monoclinic space group $P2_1/n$. Data reduction was carried out with locally written software, and included correction for L_p effects and standard reflection intensity variations; 5 [3 for **2**] standard reflections were remeasured every 60 min of X-ray exposure time and varied by up to 3% in intensity. The variation of standard reflections was also used, together with normal counting statistics, to estimate standard deviations of intensities. A semi-empirical absorption correction was applied for each structure based on sets of equivalent reflections measured at a range of azimuthal angles.[39]

Structure solution and refinement. Programs used (SHELXS 86, SHELXL 93, SHELXTL/PC) were all written by G. M. Sheldrick.[39] Atoms not revealed by initial structure solution (Patterson synthesis for compound **2**, direct methods for **7**, **8**, **11–13**) were subsequently located from difference syntheses. Least-squares refinement was based on F^2 values for all measured reflections except for any flagged for potential systematic errors, usually because of large negative measured F^2 values. Weighted indices R' are based on F^2 for all data, while R values are based on F values of 'observed' data only (for comparison with conventional refinements on F). The weighting scheme for refinement was of the form $w^{-1} = \sigma^2(F_o^2) + (aP)^2 + bP$, where P is $(F_o^2 + 2F_c^2)/3$, F_o^2 being replaced in this expression by zero if it is negative. An isotropic extinction coefficient was refined for each of the structures but was found to be negligible in all cases and was omitted in the final cycles of refinement.

Hydrogen atoms were included in geometrical positions using a riding model for all structures except **13**, which was

substantially disordered. For structures **2** and **12** the methyl hydrogens were allowed to rotate as a rigid group to find the best fit to the local electron density. Hydrogen isotropic displacement parameters were set to be 150% of those of the carrier atoms [120% for **8**]; other atoms were refined anisotropically.

For structures **2**, **7**, **8**, **11** and **12** the largest residual peaks in the electron density maps were close to either the metal atoms or the halides. For structure **13** the largest peaks were observed close to the disordered dmpe ligands. All shifts in the final cycles were < 0.003 of the corresponding e.s.d. values.

The structure of **13** was substantially disordered, although this was successfully resolved. The dmpe ligand bonded to Sb(1) is disordered over two sets of positions with atoms P(1)/P(1A), P(2)/P(2A), C(1)/C(1A) and C(5)/C(5A) being common to each part of the disorder. The sites for atoms P(1), P(2) and C(1)–C(6) have a refined occupancy of 55(4)%, while the occupancy of the sites P(1A), P(2A) and C(1A)–C(6A) is 45(4)%. Atoms C(2) and C(2A) were refined isotropically, while the remaining atoms in this dmpe ligand were refined anisotropically, with atoms C(4) and C(4A) restrained to approximately isotropic behaviour. The fragment containing Sb(2) was also highly disordered. The Br atoms occupy two sets of positions, each constrained to have equal occupancy. There are two sets of positions for the dmpe ligand with atoms P(3)/P(3A), C(7)/C(7A) and C(9)/C(9A) being common to both. The set of positions P(3), P(4) and C(7)–C(12) have 52(2)% occupancy, while the other set of positions have 48(2)% occupancy. All atoms in this fragment were refined anisotropically, with C(8), C(10) and C(11) being restrained to approximately isotropic behaviour.

Additional material available from the Cambridge Crystallographic Data Centre comprises H-atom coordinates, thermal parameters and remaining bond lengths and angles.

Acknowledgements

We thank the SERC for a research grant (W. C.) and a studentship (N. L. P.) and N. C. N. thanks the Royal Society for additional supporting funds. We also thank Professor V. C. Gibson for helpful discussions.

References

1 C. A. McAuliffe (editor), *Transition Metal Complexes of Phosphorus, Arsenic and Antimony Ligands*, Macmillan, London, 1973.
2 W. Levason and C. A. McAuliffe, *Coord. Chem. Rev.*, 1976, **19**, 173; N. C. Norman and N. L. Pickett, *Coord. Chem. Rev.*, in preparation.
3 R. R. Holmes and E. F. Bertaut, *J. Am. Chem. Soc.*, 1958, **80**, 2980.
4 J. C. Summers and H. H. Sisler, *Inorg. Chem.*, 1970, **9**, 862.
5 W. Clegg, R. J. Errington, G. A. Fisher, M. E. Green, D. C. R. Hockless and N. C. Norman, *Chem. Ber.*, 1991, **124**, 2457.
6 W. Clegg, R. J. Errington, R. J. Flynn, M. E. Green, D. C. R. Hockless, N. C. Norman, V. C. Gibson and K. Tavakkoli, *J. Chem. Soc., Dalton Trans.*, 1992, 1753.
7 W. Clegg, M. R. J. Elsegood, V. Graham, N. C. Norman and N. L. Pickett, *J. Chem. Soc., Dalton Trans.*, 1993, 997.
8 H. A. Kaul, D. Greissinger, W. Malisch, H. P. Klein and U. Thewalt, *Angew. Chem., Int. Ed. Engl.*, 1983, **22**, 60.
9 B. Sigwarth, U. Weber, L. Zsolnai and G. Huttner, *Chem. Ber.*, 1985, **118**, 3114.
10 G. A. Fisher and N. C. Norman, *Adv. Inorg. Chem.*, in the press.
11 W. Clegg, R. J. Errington, G. A. Fisher, D. C. R. Hockless, N. C. Norman, A. G. Orpen and S. E. Stratford, *J. Chem. Soc., Dalton Trans.*, 1992, 1967; W. Clegg, R. J. Errington, G. A. Fisher, R. J. Flynn and N. C. Norman, *J. Chem. Soc., Dalton Trans.*, 1993, 637 and refs. therein.
12 N. C. Norman, *Phosphorus Sulfur*, in the press.
13 S. Pohl, W. Saak, R. Lotz and D. Haase, *Z. Naturforsch., Teil B*, 1990, **45**, 1355.
14 W. Clegg, L. J. Farrugia, A. McCamley, N. C. Norman, A. G. Orpen, N. L. Pickett and S. E. Stratford, *J. Chem. Soc., Dalton Trans.*, 1993, 2579.
15 F. Lazarini and S. Milicev, *Acta Crystallogr., Sect. B*, 1976, **32**, 2873.
16 W. Clegg, N. C. Norman and N. L. Pickett, *Acta Crystallogr., Sect. C*, 1994, **50**, 36 and refs. therein; see for example, M. R. Bermejo, A. Fernandez, M. Gayoso, A. Castineiras, W. Hiller and J. Strahle, *Polyhedron*, 1988, **7**, 2561; A. Castineiras, M. R. Bermejo, A. Garcia-Deibe and W. Hiller, *Acta Crystallogr., Sect. C*, 1991, **47**, 1738.
17 J. H. Wengrovius, R. R. Schrock and C. S. Day, *Inorg. Chem.*, 1981, **20**, 1844.
18 F. A. Cotton, M. P. Diebold and P. A. Kibala, *Inorg. Chem.*, 1988, **27**, 799.
19 F. A. Cotton, M. Shang and W. A. Wojtczak, *Inorg. Chem.*, 1991, **30**, 3670.
20 M. E. Riehl, S. R. Wilson and G. S. Girolami, *Inorg. Chem.*, 1993, **32**, 218.
21 F. A. Cotton, P. A. Kibala and W. A. Wojtczak, *Inorg. Chim. Acta*, 1990, **177**, 1.
22 F. A. Cotton, J. Liu and T. Ren, *Inorg. Chim. Acta*, 1994, **215**, 47.
23 A. P. Sattelberger, R. B. Wilson and J. C. Huffman, *J. Am. Chem. Soc.*, 1980, **102**, 7111; *Inorg. Chem.*, 1982, **21**, 2392.
24 F. A. Cotton, J. L. Eglin, R. L. Luck and K. Son, *Inorg. Chem.*, 1990, **29**, 1802.
25 J. T. Barry, S. T. Chacon, M. H. Chisholm, V. F. Distasi, J. C. Huffman, W. E. Streib and W. G. Van der Sluys, *Inorg. Chem.*, 1993, **32**, 2322.
26 F. A. Cotton and S. K. Mandal, *Inorg. Chem.*, 1992, **31**, 1267.
27 F. A. Cotton, M. Matusz and R. C. Torralba, *Inorg. Chem.*, 1989, **28**, 1516.
28 F. A. Cotton, S.-J. Kang and S. K. Mandal, *Inorg. Chim. Acta*, 1993, **206**, 29.
29 P. Sobota, J. Ejfler, S. Szafert, K. Szczegot and W. Sawka-Dobrowolska, *J. Chem. Soc., Dalton Trans.*, 1993, 2353.
30 G. B. Deacon, T. Feng, S. Nickel, B. W. Skelton and A. H. White, *J. Chem. Soc., Chem. Commun.*, 1993, 1328.
31 F. A. Cotton, J. L. Eglin and C. A. James, *Inorg. Chem.*, 1993, **32**, 687.
32 R. Poli and J. C. Gordon, *J. Am. Chem. Soc.*, 1992, **114**, 6723.
33 R. Poli and R. C. Torralba, *Inorg. Chim. Acta*, 1993, **212**, 123.
34 W. Clegg, M. R. J. Elsegood, N. C. Norman and N. L. Pickett, following paper.
35 R. A. Wheeler and P. N. V. P. Kumar, *J. Am. Chem. Soc.*, 1992, **114**, 4776.
36 W. S. Sheldrick and C. Horn, *Z. Naturforsch., Teil B*, 1989, **44**, 405.
37 W. Clegg, *Acta Crystallogr., Sect. A*, 1981, **37**, 22.
38 J. Cosier and A. M. Glazer, *J. Appl. Crystallogr.*, 1986, **19**, 105.
39 G. M. Sheldrick, SHELXTL/PC Users manual, Siemens Analytical Instruments Inc., Madison, WI, 1990; SHELXS 86, program for crystal structure solution, University of Göttingen, 1986; SHELXL 93, program for crystal structure refinement, University of Göttingen, 1993.

Received 15*th February* 1994; *Paper* 4/00915K